Crystal structure of the human prion protein reveals a mechanism for oligomerization

Karen J. Knaus[1,2], Manuel Morillas[3], Wieslaw Swietnicki[3], Michael Malone[4], Witold K. Surewicz[3,5,6] and Vivien C. Yee[1,2,4]

[1]Department of Molecular Cardiology and Center for Structural Biology, Lerner Research Institute, Cleveland Clinic Foundation, 9500 Euclid Avenue NB20, Cleveland, Ohio 44195, USA. [2]Department of Chemistry, Cleveland State University, Cleveland, Ohio 44115, USA. Departments of [3]Pathology, [4]Pharmacology, [5]Chemistry and [6]Physiology and Biophysics, Case Western Reserve University, 10900 Euclid Avenue, Cleveland, Ohio 44106, USA.

The pathogenesis of transmissible encephalopathies is associated with the conversion of the cellular prion protein, PrP^{C}, into a conformationally altered oligomeric form, PrP^{Sc}. Here we report the crystal structure of the human prion protein in dimer form at 2 Å resolution. The dimer results from the three-dimensional swapping of the C-terminal helix 3 and rearrangement of the disulfide bond. An interchain two-stranded antiparallel β-sheet is formed at the dimer interface by residues that are located in helix 2 in the monomeric NMR structures. Familial prion disease mutations map to the regions directly involved in helix swapping. This crystal structure suggests that oligomerization through 3D domain-swapping may constitute an important step on the pathway of the $PrP^{C} \rightarrow PrP^{Sc}$ conversion.

Prion diseases, or spongiform encephalopathies, are an intriguing group of neurodegenerative diseases that include scrapie in sheep, bovine spongiform encephalopathy (BSE) in cattle, and Creutzfeldt-Jakob disease (CJD), Gerstmann-Sträussler-Scheinker disease, fatal familial insomnia and kuru in humans[1,2]. These diseases can arise sporadically, be inherited or be transmitted by an infectious agent that, according to the 'protein only' hypothesis, is the abnormal form of the prion protein. The critical event in disease transmission is believed to be the conversion of a monomeric, protease-sensitive prion protein, PrP^{C}, into a protease-resistant, oligomeric form, PrP^{Sc}. The emergence of new variant CJD (nvCJD), a transmissible spongiform encephalopathy believed to be spread by dietary exposure to BSE-tainted beef[3], has brought a special urgency to the study of the PrP^{C} to PrP^{Sc} conversion. Spectroscopic data show that PrP^{C} is highly α-helical, whereas PrP^{Sc} has a largely β-sheet structure[4], indicating that the conversion to PrP^{Sc} involves a major conformational transition. Solution NMR studies of recombinant prion proteins from four species[5–8] gave similar, predominantly α-helical, monomeric folds which were presumed to represent the PrP^{C} structure. Here we present the 2.0 Å resolution crystal structure of a recombinant human prion protein in a dimeric form. The structure reveals an unexpected three-dimensional (3D) domain swapping that may provide a mechanism for protein oligomerization. A conformational switch region is located at the dimer interface.

The crystal structure of the human prion protein is a dimer

The human prion protein used for crystallization (residues 90–231) was expressed in *Escherichia coli* and oxidatively refolded[9,10] to give soluble protein. This procedure provided monomeric, refolded protein containing an intramolecular disulfide bond[11,12]; its NMR structure was reported[7,13]. This recombinant fragment[11], as well as the shorter (121–231) version (unpublished data), can undergo a conformation transition from α-helical to a β-sheet-rich PrP^{Sc}-like oligomeric structure. Because molecular replacement calculations using the mouse and hamster prion protein NMR structures available at the time were unsuccessful, phases were determined by heavy atom methods using a single platinum derivative (Table 1). Refinement against data to 2.0 Å resolution yield R-factor and R_{free} values of 0.206 and 0.253, respectively, and a final protein model consist-

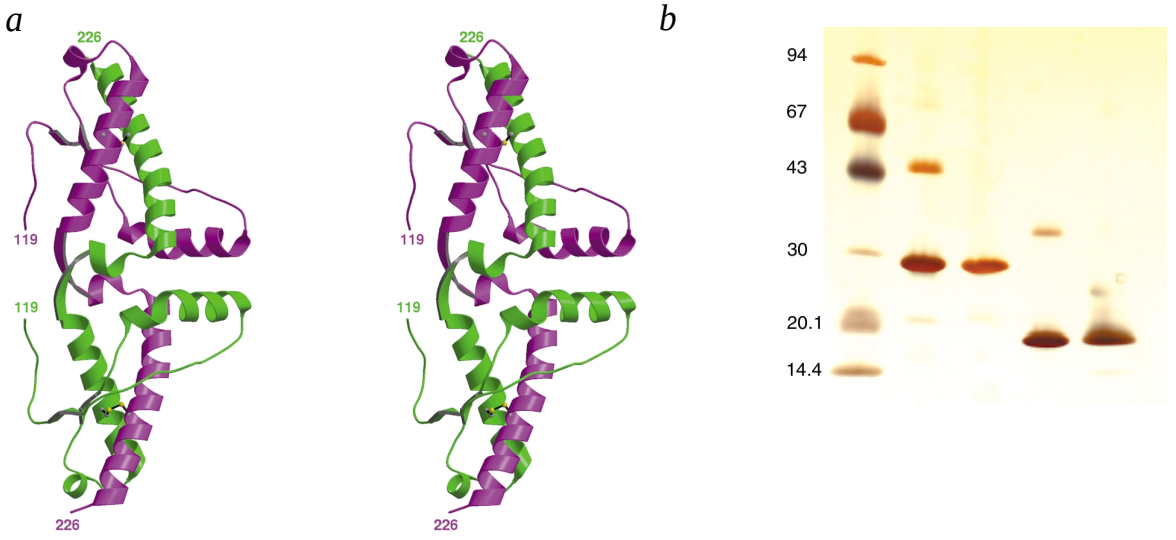

Fig. 1 The human prion protein dimer. ***a***, Stereo view ribbon diagram of the human prion protein dimer crystal structure. The two peptide chains are in green and pink, with their N- and C- termini labeled; the two interchain disulfide bridges are shown as ball-and-stick structures. ***b***, Silver-stained SDS-PAGE showing covalent dimers of the human prion protein. From the left, the lanes are: molecular weight markers spanning 14.4–94 kDa, recombinant human prion protein (23–231) under nonreducing and reducing conditions, and recombinant human prion protein (90–231) under nonreducing and reducing conditions.

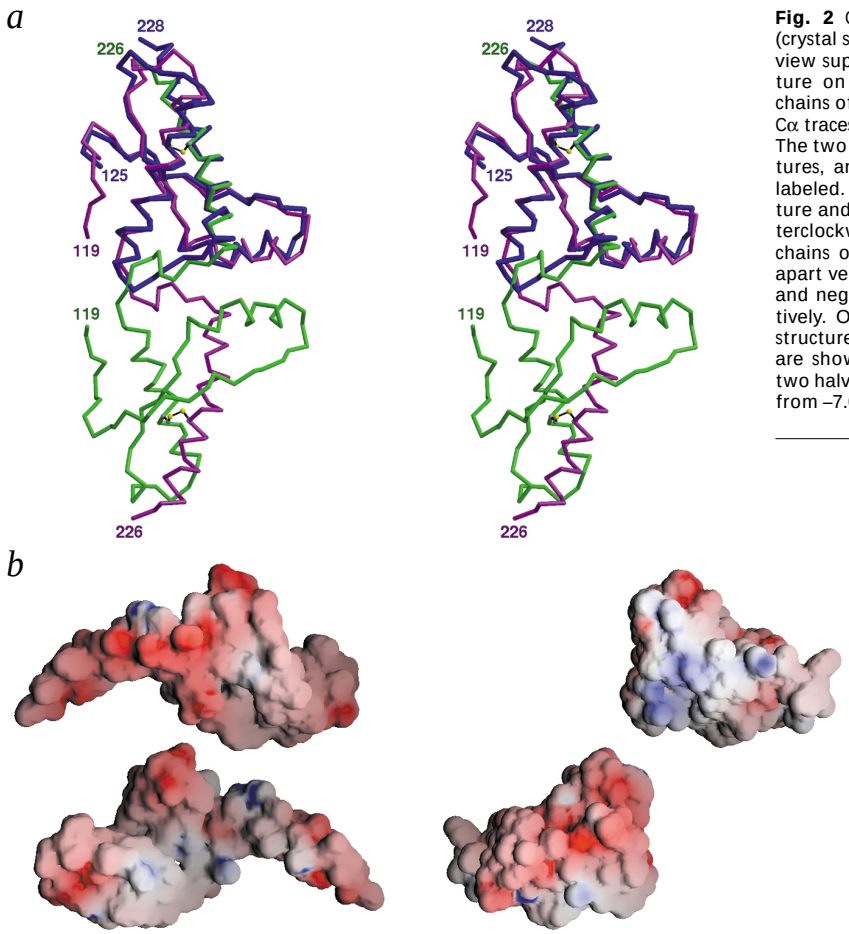

Fig. 2 Comparison of the human prion protein dimer (crystal structure) and monomer (NMR structure). ***a***, Stereo view superposition of the monomeric solution NMR structure on the dimeric crystal structure. The two peptide chains of the crystal structure are drawn as green and pink Cα traces with the NMR structure (PDB code 1QLX) in blue. The two disulfide bridges are shown as ball-and-stick structures, and the N- and C-termini for all three chains are labeled. ***b***, Electrostatic surfaces of the dimeric crystal structure and the monomeric NMR structure, viewed 90° counterclockwise relative to (*a*). On the left, the two peptide chains of the dimeric crystal structure have been pulled apart vertically for individual surface calculations; positive and negative surface charges are in blue and red, respectively. On the right**,** two views of the monomeric NMR structure related by a 180° rotation about the vertical axis are shown, which correspond to the orientations of the two halves of the crystal structure dimer. The energy scale is from –7.0 to +7.0 for the surface potential.

ing of residues Gly 119–Tyr 226. SDS-PAGE under reducing conditions showed that the dissolved crystals contain protein with a lower apparent molecular weight than the protein stock solution used for crystallization. Mass spectrometric peaks for dissolved crystals are consistent with N-terminally truncated protein corresponding to the beginning of the ordered structure observed in the crystal. Very slow cleavage is likely caused by residual protease contaminants that were incompletely removed during protein purification. The proteolytic susceptibility of the N-terminal region is consistent with solution NMR studies of recombinant prion proteins, which revealed that this region is unstructured[5–8].

The most dramatic feature of the prion protein crystal is the dimeric structure, with the two polypeptide chains related by crystallographic two-fold symmetry (Fig. 1*a*). Near the N-terminus of each chain, there are four main chain hydrogen bonds between two short stretches of antiparallel β-sheet. There are three long α-helices in the rest of each monomer. Helix 1 (Ser 143–Tyr 157) is at the dimer interface, and helix 2 (Asn 171–Thr 188) is linked to the C-terminal helix 3 (Thr 199–Tyr 225) from the other polypeptide chain in the dimer by an interchain disulfide bond. SDS-PAGE confirmed that the dissolved crystals contain covalently dimerized protein: the dimer band was observed under nonreducing conditions but disappeared when 2-mercaptoethanol was added. By comparison, the same gels showed that covalent dimer was absent in a freshly prepared sample of the purified protein. Incubation of the protein in solution at room temperature results in a time-dependent appearance of a minor band corresponding to prion protein dimer. This dimeric component was also observed (in the presence of protease inhibitors) for the intact PrP fragment (90–231) as well as the full length PrP (23–231) (Fig. 1*b*). The dimer can be removed by column chromatography but reappears upon further incubation of the protein at room temperature. Altogether, the electrophoretic data indicate that the truncation and dimerization of the initially monomeric protein occurs during the crystallization process, which takes several weeks. Dimerization appears to be an equilibrium process: dimerized protein selectively crystallizes, driving further formation of covalent dimer to feed crystal growth. A second crystal form of the human prion protein, diffracting to only 2.9 Å resolution, also gave a similar dimer structure.

Comparison of the dimeric and monomeric structures

Solution NMR studies of mammalian prion proteins have been carried out with full length (23–230/231) and truncated (90–231 and 121–230/231) polypeptides[5–8,13]. All show similar monomeric folds that are structured from about residue 125. Comparison with the solution NMR structure of the human prion protein monomer[7] reveals that the crystal structure is best described as a 3D domain-swapped dimer (Fig. 2*a*). By superimposing Cα atoms for residues 125–190 from one monomer and residues 197–225 from the second monomer onto the corresponding atoms of the NMR structure, a calculated r.m.s. deviation of 1.5 Å indicates that the packing of interchain helix 3 in the crystal structure is very similar to its intrachain packing in the NMR structure. The structural features that differ the greatest are helix 3, which packs against helix 2 from the other monomer in

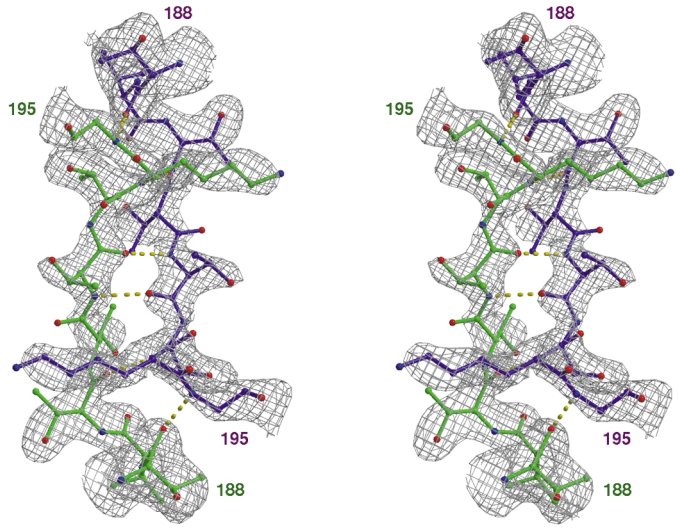

Fig. 3 Stereo view of 29.0–2.0 Å resolution omit $|F_o| - |F_c|$ electron density contoured at 2 σ for the two antiparallel β-strands containing residues Thr 188–Gly195 in the switch region at the prion protein dimer interface. Electron density is shown in gray contour with the bonds from the two peptide chains in green and pink, respectively; residues 188 and 195 in each chain are labeled. The six main chain hydrogen bonds are shown as dashed yellow lines (Thr188 O–Gly195 N, Thr190 O–Lys194 N and Thr192 O–Thr192 N; the other three bonds are related by crystallographic two-fold symmetry).

the dimer rather than against its own polypeptide chain in the crystal structure, and the switch region consisting of residues Val 189–Phe 198, which crosses the dimer interface and connects the core of each monomer to the extended, swapped helix 3. In the NMR-derived structure of the monomer, helix 2 ends at Gly 195; in the crystal structure of the dimer, the last turn of helix 2 has unwound to Val 189. In both the monomer and dimer structures, helix 3 begins at Thr 199. The intervening residues Thr 190–Phe 198 are extended in the NMR structure, whereas the switch region between helices 2 and 3 forms a short stretch of β-strand followed by a single helical turn in the crystal structure. In addition to the conformational change in the switch region, the other parts of the crystal structure that are different from that determined by NMR are (i) the flexible termini, especially the N-terminal residues Gly 119–Gly 124, which are observed in the electron density of the crystal structure but are disordered in the NMR structure; (ii) residues Arg 164–Asp 178 that comprise a surface loop and the N-terminus of helix 2; and (iii) helix 1, which forms part of the dimer interface. The Gly 119–Gly 124 segment, which is unstructured in NMR studies, is stabilized in the crystal structure by packing against helix 2 and the switch region.

Calculated surface electrostatic distributions are very different for the monomeric NMR structure and the dimeric crystal structure (Fig. 2*b*). These differences may be of functional relevance because they could affect the interaction of prion protein with cellular membranes[5,9] and other macromolecular partners. The monomeric NMR structure has a highly polarized surface and a calculated molecular dipole of 290 Debye. In the crystal structure, each monomer gives a smaller molecular dipole of 89 Debye, which, through the two-fold symmetry of the dimer, partially cancel each other to give a negligible net molecular dipole of 37 Debye. Because the distribution of surface electrostatics is much more polarized in the monomer than in the dimer, any functional relevance of surface electrostatics for monomeric PrP^C may be different than for an oligomeric PrP^{Sc} that may form by 3D domain-swapping.

The observation of a 3D domain-swapped dimer in the crystal structure requires that a dramatic conformational transition must have occurred: the intrachain disulfide bonds in the monomers must be reduced, the two helices 3 must swing out across the dimer interface to swap and pack against the other half of the dimer, and the two disulfide bridges must re-form between polypeptide chains. Three-dimensional domain-swapping is a mechanism of oligomerization for a variety of proteins[14,15] and interchain disulfides in domain-swapped structures are not unprecedented[16]. The switch region between helices 2 and 3 in the prion crystal structure consists of a short stretch of β-strand and one turn of helix, and results partly from the conversion of the last turn of helix 2, as observed in the NMR structure, to the β-strand observed in the crystal structure. The two β-strands in the switch regions of the two polypeptide chains come together at the dimer interface to form a two-stranded, antiparallel β-sheet with six main chain hydrogen bonds (Fig. 3). Thus, the dimer interface observed in the crystal structure has several components that include helix 1–helix 1 interactions and the interchain antiparallel β-sheet, neither of which have counterparts in the monomeric NMR structure, and helix 2–helix 3 packing, which is present in both monomeric and dimeric structures. There are also additional intrachain van der Waals and electrostatic interactions between the switch region and helix 1 in the 3D domain-swapped dimeric crystal structure that are not possible in the monomeric NMR structure. Ignoring the interchain helix 2–helix 3 packing, the dimer interface is characterized by a total buried accessible surface area of 2,076 $Å^2$ and a complementarity index of 0.683, both of which are within the expected range

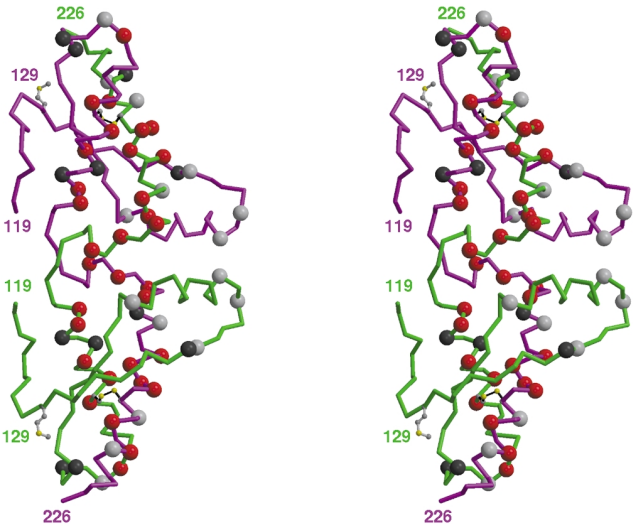

Fig. 4 Mapping of residues relevant to disease transmission to the prion dimer structure, shown as a stereo Cα trace. The 17 amino acids altered in familial spongiform encephalopathies (reviewed in reference 18 and at *http://www.mad-cow.org/prion_point_mutations.html*) are represented as large red Cα spheres and are all located in the swapped helix 3, its flanking helix 2 or the switch region between them. The side chain of Met 129, where Val 129 is a marker for (nv)CJD, is shown in ball-and-stick. Seven amino acids, which are nonconserved between human and bovine, and eight additional amino acids, which are nonconserved between human and mouse or hamster proteins, are shown as large Cα spheres in dark and light gray, respectively.

Table 1 Summary of crystallographic data

Data measurement			
Crystal	form 1 native	form 1 Pt	form 2 native
Source	APS 19ID	APS 19ID	NSLS X25
Wavelength (Å)	1.0688	1.0717	1.1000
Space group (Å)	$C222_1$		$I4_122$
a	85.4	86.4	72.2
b	85.7	85.9	
c	40.5	40.4	158.0
Bijvoets merged	yes	no	yes
Unique reflections	10,069	7,160	4,367
Redundancy	7.8	4.6	6.5
Resolution (Å)[1]	30–2.0 (2.07–2.0)	30–2.8 (2.9–2.8)	100–2.9 (3.0–2.9)
R_{sym} (%)[1,2]	4.8 (23.9)	6.0 (22.4)	6.2 (11.7)
Completeness (%)[1]	96.7 (84.8)	99.7 (99.1)	87.8 (59.1)
$I / \sigma (I)$[1]	36 (5.5)	23 (6.6)	23 (6.2)
Phasing power[3]		1.84	
R_{cullis}[4]		0.798	
Refinement (form 1)			
Resolution (Å)		30–2.0	
Number of reflections, $F > 0 \sigma$		10,069	
Reflections excluded for cross-validation (%)		7	
R-factor[5]		0.206	
R_{free}[5]		0.253	
Deviations from ideality			
R.m.s. deviations			
Bond length (Å)		0.008	
Bond angle (°)		1.17	
B-factors, bonded main chain atoms (Å^2)		2.1	
B-factors, bonded side chain atoms (Å^2)		3.0	
Ramachandran plot			
Most favored (% residues)		95	
Disallowed (% residues) 0			

[1]Values in parentheses are for highest resolution shell.
[2]$R_{sym} = \sum |I_{obs} - I_{ave}| / \sum I_{ave}$.
[3]Phasing power = r.m.s. ($|F_H| / E$), where E is the residual lack of closure for acentric reflections.
[4]$R_{cullis} = \sum ||F_{PH}| \pm |F_P| - |F_H|| / \sum ||F_{PH}| \pm |F_P||$ for centric reflections.
[5]R-factor = $\sum |F_o - F_c| / \sum F_o$ and R_{free} = R-factor calculated for test set of reflections not used in refinement (7% comprising 728 reflections for crystal form 1 and 325 for crystal form 2).

for functionally relevant protein–protein interactions[17,18]. With the helix 3 packing included in the calculations, the total buried accessible surface area and complementarity index increase to 6,505 Å^2 and 0.738, respectively, and are characteristic of a very extensive, highly complementary interface.

Implications of 3D domain-swapping

All of the amino acids altered in familial human spongiform encephalopathies[19] are concentrated in the crystallized prion fragment in the swapped helix 3, the neighboring helix 2 (against which helix 3 packs) and the switch region between these two helices (Fig. 4). The altered residues are located in the switch region or at the C-terminus of helix 2, next to the β-strand formed from the unwinding of the final helical turn observed in the monomeric NMR structure, and may affect the equilibrium between the monomer and the dimer. The other altered residues are located in regions of helices 2 and 3 that form the closed interface and may affect the rate of dimer formation. In contrast, the nonconserved residues, which are divergent among the prion protein sequences from different mammals and thus may be responsible for the 'species barrier', are distributed throughout the dimer: in the swapped helix 3, in helix 1 at the dimer interface and in some exposed segments (Fig. 4). The divergent residues located in helix 1 may affect the monomer/dimer equilibrium, whereas those in helix 3 may affect the rate of dimer formation. Although helix 3 packs intimately against the core of the other monomer, only Asp 202 and Arg 220, which are located at either end of helix 3, form interchain hydrogen bonds that confer specificity to the interaction. Three of the four residues (Ile 215, Glu 219 and Gln 172)[20] believed to be important for binding to Protein X, a postulated binding protein[20], are concentrated near Arg 220. This observation suggests that the Protein X-binding residues may also affect helix 3 swapping.

This crystal structure provides the first high resolution view of a structural transition for the prion protein. The mechanism of PrP^{Sc} formation under physiological conditions is at present unknown. However, within the context of the nucleation dependent polymerization model of prion propagation[21], the presence of dimers could accelerate the formation of a nucleus that acts as a seed for the formation of highly ordered PrP^{Sc} aggregates. The role of prion protein dimerization in the pathogenesis of spongiform encephalopathies was previously postulated based on the observation that covalently-linked PrP dimers are present in mouse neuroblastoma cells and in scrapie-infected hamster brain[22]. The present finding that helix swapping may provide an effective mechanism for oligomerization of the prion protein is especially intriguing when combined with the recent report that the amyloidogenic protein human cystatin C can also form a 3D domain-swapped dimer[15]. Observation of the cystatin C dimer led to the speculation that amyloids may form by an oligomeric chain of head-to-tail 3D domain-swapped monomers. In view of the present data, a similar general hypothesis may be also applicable to oligomerization of the prion protein. However, additional conversion of some α-helices to β-sheets would be expected for formation of mature PrP^{Sc}. Furthermore, in the case of the prion protein, the transition from the monomer to the 3D domain-swapped dimer involves the reduction and reformation of two disulfide bonds, which occurs with no reducing agent added to the protein buffer or crystallization solution. Although the mechanism for the disulfide swapping is currently unknown, it likely involves some degree of transient protein unfolding, given the molten globule-like properties of the reduced recombinant prion protein[9].

The location of one of the N-linked glycosylation sites, Asn 197, in the switch region of the nonglycosylated dimeric crystal structure is intriguing. The Asn 197 side chain is only partially solvent-exposed in the dimeric crystal structure and much more exposed in the monomeric NMR structure. Glycosylation of this residue would likely affect the relative stabilities of monomeric and 3D domain-swapped prion protein oligomers. The finding that helix swapping can provide a mechanism for oligomerization of prion protein has potentially important

implications for the pathogenesis, diagnosis and treatment of spongiform encephalopathies. In particular, disruption of the dimerization interface emerges as a well-defined target for the design of drugs that can interfere with the conformational transition and oligomerization of the prion protein and, thus, inhibit formation of the pathogenic PrP^{Sc} isoform. On the diagnostic front, identification of potential epitopes that are exposed in the prion protein monomer but buried in the dimeric structure should facilitate efforts to obtain PrP^{Sc}-specific antibodies for early detection of spongiform encephalopathies.

Methods

Expression and crystallization. Human prion protein (90–231) was expressed in *E. coli*, refolded and purified as described[9,10]. Crystals, obtained at 20 °C by vapor diffusion with protein at 5 mg ml^{-1} and reservoir consisting of 0.1 M Tris-HCl, pH 8, 3 M NaCl and 5 mM $CdCl_2$, were stabilized with 2,4-dimethyl-2,4-pentanediol prior to data collection at –180 °C. Silver-stained SDS-PAGE with protein stock solution, dissolved crystals and crystallization mother liquor (all under reducing and nonreducing conditions) revealed that the crystallized protein is cleaved and dimerized (data not shown). MALDI-TOF mass spectrometric analysis of protein stock solution and dissolved crystals confirmed the proteolysis and identified a molecular weight of 13.1 kDa for the latter. This is consistent with the ordered crystal structure that is N-terminally truncated at residue Gly 119, indicating that the protein has been proteolysed at the N-terminus. The crystals have unit cell dimensions of 85.4 Å × 85.7 Å × 40.5 Å, space group $C222_1$ and one polypeptide chain in the asymmetric unit. They diffract to 2.0 Å resolution. A second crystal form also containing one proteolytically cleaved peptide chain in the asymmetric unit was grown from similar conditions but at pH 7. This crystal has unit cell dimensions of 72.2 Å × 72.2 Å × 158.0 Å and space group $I4_122$ but diffracts to only 2.9 Å resolution.

Structure determination. For crystal form 1, preliminary crystal characterization and heavy atom derivative testing were carried out at ALS beamline 5.0.1 and NSLS beamline X25. Diffraction data were measured at APS beamline 19ID from a native crystal and from a heavy atom derivative obtained by soaking a crystal in 5 mM K_2PtCl_4 for 2 d; the native and optimized SIRAS data were processed with HKL[23]. Phasing calculations were carried out with SOLVE[24] and SHARP[25] and followed by solvent flattening with DM[26], which improved the figure of merit from 0.52 to 0.64, resulting in interpretable electron density for building the structure using O[27]. Iterative cycles of refinement using CNS[28] and model rebuilding resulted in an R-factor of 0.206 and R_{free} of 0.253 to 2.0 Å resolution. The final model contains protein residues 119–226 of one monomer, two cadmium ions, one chloride ion and 113 water molecules; the second monomer in the dimer is related by two-fold crystallographic symmetry. Neither cadmium ion is located at the dimer interface nor near the switch region; thus, they are not likely to be important in the dimer formation. One cadmium ion is bound to three water molecules and residues His 140 and Asp 147 within the same monomer, apparently to stabilize a surface loop forming a crystal contact. The second cadmium ion is coordinated by five water molecules and His 177, an exposed helix 2 residue that is at a crystal contact. Data for crystal form 2 were measured at NSLS beamline X25; the structure was solved by molecular replacement. Crystal form 2 contains a similar crystallographic dimer and was refined against data to 2.9 Å resolution to give an R-factor and R_{free} of 0.215 and 0.291, respectively. All discussions and figures pertain to the higher resolution crystal form 1 structure. Data processing, heavy atom phasing and model refinement statistics are given in Table 1. Figures were generated with MOLSCRIPT[29], BOBSCRIPT[30] and RASTER3D[31]. Surface electrostatics and molecular dipoles were calculated using GRASP[32].

Coordinates. Coordinates and diffraction data have been deposited in the Protein Data Bank (accession code 1I4M).

Acknowledgments

Diffraction data were measured at APS beamline 19-ID and at ALS beamline 5.0.2., both supported by the US DOE, and at BNL NSLS beamline X25, supported by the U.S. DOE and the NIH. We are grateful to the CCF/LRI Computer Core for facilities support, to S. Ginell and T. Earnest for beamline support and especially to F. van den Akker for many helpful discussions. This work was supported by grants from the NSF and AHA to V.C.Y. and from the NIH to W.K.S.

Correspondence should be addressed to V.C.Y. *email: yeev@ccf.org*

Received 30 April, 2001; accepted 10 July, 2001

1. Prusiner, S.B. *Proc. Natl. Acad. Sci. USA* **95**, 13363–13383 (1998).
2. Horwich, A.L. & Weissman, J.S. *Cell* **89**, 499–510 (1997).
3. Bruce, M.E. *et al. Nature* **389**, 498–501 (1997).
4. Caughey, B.W. *et al. Biochemistry* **30**, 7672–7680 (1991).
5. Riek, R. *et al. Nature* **382**, 180–182 (1996).
6. Donne, D.G. *et al. Proc. Natl. Acad. Sci. USA* **94**, 13452–13457 (1997).
7. Zahn, R. et al. *Proc. Natl. Acad. Sci. USA* **97**, 145–150 (2000).
8. Lopez, G.F., Zahn, R., Riek, R. & Wuthrich, K. *Proc. Natl. Acad. Sci. USA* **97**, 8334–8339 (2000).
9. Morillas, M., Swietnicki, W., Gambetti, P. & Surewicz, W.K. *J. Biol. Chem.* **274**, 36859–36865 (1999).
10. Zahn, R., von Schroetter, C. & Wuthrich, K. *FEBS Lett.* **417**, 400–404 (1997).
11. Swietnicki, W., Morillas, M., Chen, S.G., Gambetti, P. & Surewicz, W.K. *Biochemistry* **39**, 424–431 (2000).
12. Maiti, N.R. & Surewicz, W.K. *J. Biol. Chem.* **176**, 2427–2431 (2001).
13. Zhang, Y., Swietnicki, W., Zagorski, M.G., Surewicz, W.K. & Sonnichsen, F.D. *J. Biol. Chem.* **275**, 33650–33654 (2000).
14. Bennett, M.J., Choe, S. & Eisenberg, D. *Proc. Natl. Acad. Sci. USA* **91**, 3127–3131 (1994).
15. Janowski, R. *et al. Nature Struct. Biology* **8**, 316–320 (2001).
16. Piccoli, R. *et al. Proc. Natl. Acad. Sci. USA* **89**, 1870–1874 (1992).
17. Lawrence, M.C. & Colman, P.M. *J. Mol. Biol.* **234**, 946–950 (1993).
18. Conte, L.L., Chothia, C. & Janin, J. *J. Mol. Biol.* **285**, 2177–2198 (1999).
19. Gambetti, P. *et al.* In *Prion biology and diseases* (ed. Prusiner, S.B.) 509–583 (Cold Spring Harbor Laboratory Press, Cold Spring Harbor, New York; 1999).
20. Kaneko, K. *et al. Proc. Natl. Acad. Sci. USA* **94**, 10069–10074 (1997).
21. Jarrett, J.T. & Lansbury, P.T., Jr. *Cell* **73**, 1055–1058 (1993).
22. Priola, S.A., Caughey, B., Wehrly, K. & Chesebro, B. *J. Biol. Chem.* **270**, 3299–3305 (1995).
23. Otwinowski, Z. & Minor, W. *Methods Enzymol.* **276**, 307–326 (1997).
24. Terwilliger, T.C. & Berendzen, J. *Acta Crystallogr. D* **55**, 849–861 (1999).
25. de la Fortelle, E. & Bricogne, G. *Methods Enzymol.* **276**, 472–494 (1997).
26. Collaborative Computational Project, Number 4. *Acta Crystallogr. D* **50**, 760–763 (1994).
27. Jones, T.A., Zou, J.Y., Cowan, S.W. & Kjeldgaard, M. *Acta Crystallogr.A* **47**, 110–119 (1991).
28. Brunger, A.T. *et al. Acta Crystallogr. D* **54**, 905–921 (1998).
29. Kraulis, P.J. *J. Appl. Crystallogr.*. **24**, 946–950 (1991).
30. Esnouf, R.M. *Acta Crystallogr. D* **55**, 938–940 (1999).
31. Merritt, E.A. & D. J. Bacon, D.J. *Methods Enzymol.* **277**, 505–524 (1997).
32. Nicholls, A., Sharp, K.A. & Honig, B. *Proteins* **11**, 281–296 (1991).